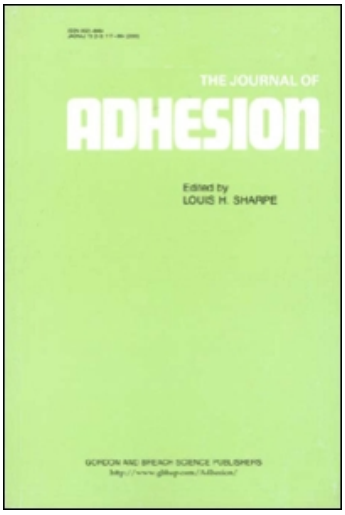

The Journal of Adhesion
Publication details, including instructions for authors and subscription information:
http://www.informaworld.com/smpp/title~content=t713453635

A Method for the Stress Analysis of Lap Joints

R. D. Adams[a]; V. Mallick[ab]
[a] Department of Mechanical Engineering, University of Bristol, Bristol, UK [b] ABB Corporate Research, Baden-Daettwil, Switzerland

To cite this Article Adams, R. D. and Mallick, V.(1992) 'A Method for the Stress Analysis of Lap Joints', The Journal of Adhesion, 38: 3, 199 — 217
To link to this Article: DOI: 10.1080/00218469208030455
URL: http://dx.doi.org/10.1080/00218469208030455

J. Adhesion, 1992, Vol. 38, pp. 199–217
Reprints available directly from the publisher
Photocopying permitted by license only

Printed in the United Kingdom

A Method for the Stress Analysis of Lap Joints

R. D. ADAMS and V. MALLICK*

Department of Mechanical Engineering, University of Bristol, Bristol BS8 1TR, UK

(Received October 16, 1991; in final form March 10, 1992)

A theory is presented for the adhesive stresses in single and double lap joints under tensile loading, while subjected to thermal stress. The formulation includes the effects of bending, shearing, stretching and hygrothermal deformation in both the adherend and adhesive. All boundary conditions, including shear stress free surfaces, are satisfied. The method is general and therefore applicable to a range of material properties and joint configurations including metal-to-metal, metal-to-CFRP or CFRP-to-CFRP. The solution is numerical and is based on an equilibrium finite element approach. Through the use of an iterative procedure, the solution has been extended to cater for non-linear adhesive materials.

KEY WORDS stress analysis; lap joints; thermal stresses; composite adherends; non-linear adhesives; finite element methods.

1 INTRODUCTION

There already exist several methods[1–7] for the stress analysis of joints. These are based either on numerical techniques, such as the finite element method, or on closed form solutions. The finite element method is capable of accurate analysis but remains expensive and requires specialist knowledge. It is, therefore, not suitable for the general adhesive technologist. Conversely, closed form methods may be easy-to-use but are less accurate. The main aim of the present analysis is to bridge the gap between the two, offering an accessible yet accurate stress analysis.

The analysis has been developed to cater for the general lap joint configuration. That is to say, the adherends may have dissimilar geometric and material properties. An attempt has been made to incorporate the influence of adhesive plasticity and hygrothermal deformation. Also included is the effect of adherend anisotropy, albeit limited to the unidirectional case.

*Present address: ABB Corporate Research, CH5405 Baden-Daettwil, Switzerland

2 MODEL: BASIC CONSIDERATIONS

Modern analytical solutions[1,3,5] for a joint usually cater for the in-plane tensile loading case. The adherends are considered as plates in bending and the adhesive as a series of tension and shear springs. Shear, in-plane (longitudinal) and out-of-plane (peel) stresses are considered in the adherend, and only shear and peel stresses are considered in the adhesive. This model for the adhesive layer can be restrictive since stresses in the longitudinal direction are ignored and stresses are often assumed to be constant across the adhesive thickness. These limitations assume particular significance when the hygrothermal response of a joint is considered. As the adhesive deforms due to hygrothermal variations, longitudinal stresses will be induced and there will be variations of stress across the adhesive, particularly at the edges.[4] Therefore, the present solution for a joint subjected to hygrothermal and tensile loading includes all three stresses, shear, peel and longitudinal, in the adhesive and also allows for their variations through the thickness.

The chosen approach is based on minimising complementary energy while satisfying equilibrium. This approach has already been employed successfully by Allman[3] and Chen and Cheng[5] and offers certain advantages over the displacement methods such as those proposed by Renton and Vinson[1] and Delale *et al.*[2] Boundary conditions, particularly at the joint ends, are easier to satisfy and in higher order solutions can be achieved with fewer variables or functions. This reduces the amount of computing power required. Another benefit, of major importance here, is that thermal stresses are easily included in a complementary energy function. For these reasons, it was decided to adopt a similar approach for the present work.

3 FORMULATION

The single lap joint (SLJ) is assumed to be in equilibrium with the edge loadings shown in Figure 1. Since the joint width is large it is reasonable to assume conditions of plane strain.

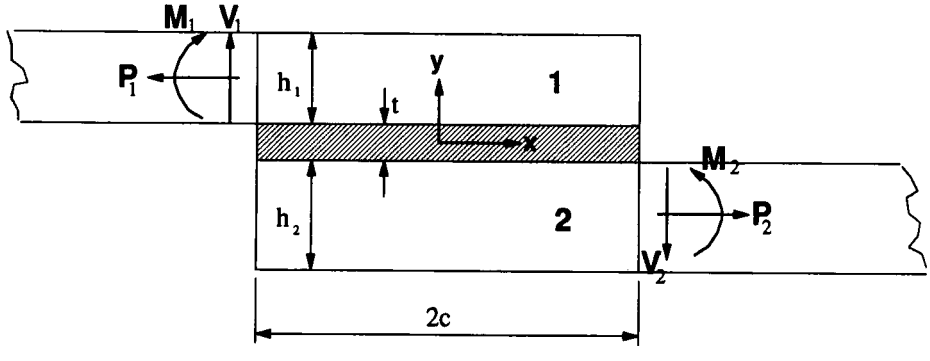

FIGURE 1 Loads at the overlap edges of a lap joint.

Therefore, the problem is reduced to one of two-dimensional elasticity where the distributions of longitudinal (σ_x), peel (σ_y) and shear (τ_{xy}) stresses need to be determined for each layer. The main simplification to be made is that σ_x in the three layers varies linearly in the transverse coordinate y. This is consistent with the classical beam-plate theory of bending and allows the stress field to be described by two independent functions of x. It will be seen later that this leads to quadratic and cubic variations in y for the shear and peel stresses, respectively.

3.1 The Single Lap Joint

The joint geometry and boundary conditions are shown in Figure 2. The x origin is located at the centre of the joint and is common for all layers. P, Q and M are the tensile load, shear load and bending moment per unit applied load, respectively. The coordinates y_1, y_2, y_a and stress components (σ_{x1}, σ_{y1}, τ_{xy1}), (σ_{x2}, σ_{y2}, τ_{xy2}), (σ_{xa}, σ_{ya}, τ_{xya}) refer to the upper adherend, lower adherend and adhesive, respectively. According to the theory of two-dimensional elasticity the stress distributions must satisfy the equations:

$$\frac{\partial \sigma_x}{\partial x} + \frac{\partial \tau_{xy}}{\partial y} = 0 \tag{1a}$$

$$\frac{\partial \sigma_y}{\partial y} + \frac{\partial \tau_{xy}}{\partial_x} = 0 \tag{1b}$$

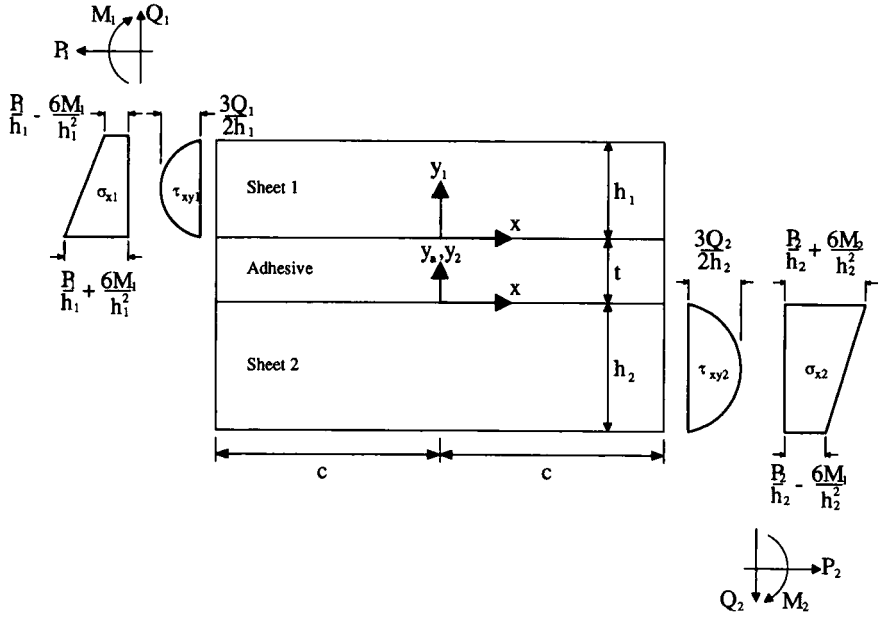

FIGURE 2 Mathematical representation of a single lap joint and its boundary conditions.

Let us consider the upper adherend first. If the longitudinal stress, σ_{x1}, varies linearly in the y direction then it can be expressed as

$$\sigma_{x1} = \phi_{11}(x) + \phi_{21}(x)\frac{y_1}{h_1} \tag{2}$$

By introducing h_1 into the equations here, large multiples of h_1 are avoided later, thus reducing numerical errors. Since $\phi_{11}(x)$ and $\phi_{21}(x)$ are functions of the x coordinate only, notation will be made more concise by dropping the (x) and writing ϕ_{11} and ϕ_{21} instead. Substituting the boundary condition that, for all y,

$$\sigma_{x1}\Big|_{x=c} = 0$$

into eqn. (2) gives the following boundary values for the stress functions ϕ_{11} and ϕ_{21}:

$$\phi_{11}\Big|_{x=c} = 0 \tag{3a}$$

$$\phi_{21}\Big|_{x=c} = 0 \tag{3b}$$

At the opposite end of the joint, the boundary conditions

$$\sigma_{x1}\Big|_{x=-c}^{y=0} = \frac{P_1}{h_1} + \frac{6M_1}{h_1^2}$$

$$\sigma_{x1}\Big|_{x=-c}^{y=h_1} = \frac{P_1}{h_1} - \frac{6M_1}{h_1^2}$$

when substituted into eqn. (2) gives

$$\phi_{11}\Big|_{x=-c} = \frac{P_1}{h_1} + \frac{6M_1}{h_1^2} \tag{3c}$$

$$\phi_{21}\Big|_{x=-c} = \frac{-12M_1}{h_1^2} \tag{3d}$$

Differentiating eqn. (2) with respect to x and substituting the result into eqn. (1a) we get

$$\frac{\partial \tau_{xy1}}{\partial y_1} = -\phi'_{11} - \phi'_{21}\frac{y_1}{h_1}$$

where a prime denotes differentiation with respect to x. Integrating this and using the boundary condition, for all x,

$$\tau_{xy1}\Big|^{y_1=h_1} = 0$$

gives the following expression for the shear stress in the upper adherend:

$$\tau_{xy1} = \phi'_{11}(h_1 - y_1) + \phi'_{21}\left[\frac{h_1}{2} - \frac{y_1^2}{2h_1}\right] \tag{4}$$

When the shear stress boundary conditions

$$\tau_{xy1}\Big|_{x=c} = 0$$

$$\tau_{xy1}\Big|_{x=-c}^{y=0} = 0$$

$$\tau_{xy1}\Big|_{x=-c}^{y=h_1/2} = \frac{-3Q_1}{2h_1}$$

are substituted into eqn. (4), the boundary values for the first derivatives of the stress functions are found to be, for all y:

$$\phi'_{11}\Big|_{x=c} = 0 \tag{5a}$$

$$\phi'_{21}\Big|_{x=c} = 0 \tag{5b}$$

$$\phi'_{11}\Big|_{x=-c} = \frac{6Q_1}{h_1^2} \tag{5c}$$

$$\phi'_{21}\Big|_{x=-c} = \frac{-12Q_1}{h_1^2} \tag{5d}$$

By substituting eqn. (4) into the second equilibrium eqn. (1b), then integrating and using the boundary condition, for all x

$$\sigma_{y1}\Big|^{y_1=h_1} = 0,$$

the peel stress is obtained as:

$$\sigma_{y1} = \phi''_{11}\left[\frac{y_1^2}{2} - h_1 y_1 + \frac{h_1^2}{2}\right] + \phi''_{21}\left[\frac{y_1^3}{6h_1} - \frac{h_1 y_1}{2} + \frac{h_1^2}{3}\right] \tag{6}$$

Similarly, for the lower adherend, the stresses are

$$\sigma_{x2} = \phi_{12} + \phi_{22}\frac{y_2}{h_2} \tag{7}$$

$$\sigma_{y2} = \phi''_{12}\left[\frac{y_2^2}{2} + h_2 y_2 + \frac{h_2^2}{2}\right] + \phi''_{22}\left[\frac{y_2^3}{6h_2} - \frac{h_2 y_2}{2} - \frac{h_2^2}{3}\right] \tag{8}$$

$$\tau_{xy2} = \phi'_{12}(-h_2 - y_2) + \phi'_{22}\left[\frac{h_2}{2} - \frac{y_2^2}{2h_2}\right] \tag{9}$$

The boundary values of the stress functions ϕ_{12} and ϕ_{22} are

$$\phi_{12}\Big|_{x=c} = \frac{P_2}{h_2} + \frac{6M_2}{h_2^2} \tag{10a}$$

$$\phi_{22}\Big|_{x=c} = \frac{12M_2}{h_2^2} \tag{10b}$$

$$\phi_{12}\Big|_{x=-c}=0 \tag{10c}$$

$$\phi_{22}\Big|_{x=-c}=0 \tag{10d}$$

and for the first derivatives

$$\phi'_{12}\Big|_{x=c}=\frac{-6Q_2}{h_2^2} \tag{11a}$$

$$\phi'_{22}\Big|_{x=c}=\frac{-12Q_2}{h_2^2} \tag{11b}$$

$$\phi'_{12}\Big|_{x=-c}=0 \tag{11c}$$

$$\phi'_{22}\Big|_{x=-c}=0 \tag{11d}$$

In the adhesive, the longitudinal stress is also assumed to vary linearly with y giving

$$\sigma_{xa}=\phi_{1a}+\phi_{2a}\frac{y_a}{t} \tag{12}$$

Now, for all y,

$$\sigma_{xa}\Big|_{x=\pm c}=0$$

therefore

$$\phi_{1a}\Big|_{x=\pm c}=0 \tag{13a}$$

$$\phi_{2a}\Big|_{x=\pm c}=0 \tag{13b}$$

Substituting eqn. (12) into equilibrium eqn. (1a) and integrating with respect to y we get

$$\tau_{xya}=-\phi'_{1a}y_a-\phi'_{2a}\frac{y_a^2}{2t}+f_1 \tag{14}$$

where f_1 is a function of x arising from the integration. The shear stress in the upper adherend and adhesive must be equal at the interface, for all x:

$$\tau_{xya}\Big|^{y_a=t}=\tau_{xy1}\Big|^{y_1=0}$$

Therefore we can set $y_a=t$ in eqn. (14) and $y_1=0$ in eqn. (9) and equate the resulting expressions to give

$$f_1=-\phi'_{12}h_2+\phi'_{22}\frac{h_2}{2} \tag{15}$$

Alternatively, we could have equated the shear stresses at the other interface:

$$\tau_{xya}\Big|^{y_a=0} = \tau_{xy2}\Big|^{y_2=0}$$

This results in the following expression for f_1:

$$f_1 = \phi'_{11}h_1 + \frac{\phi'_{21}h_1}{2} + \phi'_{1a}t + \frac{\phi'_{2a}t}{2} \tag{16}$$

Equating the right hand sides of eqns. (15) and (16) then integrating, we have

$$-\frac{\phi_{22}h_2}{2} + \phi_{12}h_2 + \phi_{11}h_1 + \frac{\phi_{21}h_1}{2} + \phi_{1a}t + \frac{\phi_{2a}t}{2} + k_1 \tag{17}$$

where k_1 is a constant of integration. Substituting the boundary values at $x = c$, (3a & b), (10a & b) and (13a & b), into eqn. (17) gives $k_1 = P_1$ while substitution of conditions at $x = -c$, (3c & d), (10c & d) and (13a & b), gives $k_1 = P_2$. Therefore the constraint

$$k_1 = P_1 = P_2 \tag{18}$$

is imposed on the system. In other words, the x forces should be in equilibrium. Therefore we can write P for both P_1 and P_2.

Substituting eqn. (14) into equilibrium eqn. (1b) and integrating with respect to y, we get

$$\sigma_{ya} = \phi_{1a}''\frac{y_a^2}{2} + \phi_{2a}''\frac{y_a^3}{6t} - f_1'y_a + f_2 \tag{19}$$

where f_2 is a function of x arising from the integration. Analogous to the shear stress, the peel stress at the adherend-adhesive interfaces must be equal, therefore, for all x,

$$\sigma_{ya}\Big|^{y_a=t} = \sigma_{y1}\Big|^{y_1=0}$$

$$\sigma_{ya}\Big|^{y_a=0} = \sigma_{y2}\Big|^{y_2=0}$$

From these conditions the following two expressions for f_2 may be derived:

$$f_2 = \frac{\phi''_{11}h_1^2}{2} + \frac{\phi''_{21}h_1^2}{3} - \frac{\phi''_{1a}t^2}{2} - \frac{\phi''_{2a}t^2}{6} + f_1't \tag{20}$$

$$f_2 = \frac{\phi''_{12}h_2^2}{2} - \frac{\phi''_{22}h_2^2}{3} \tag{21}$$

Substituting eqn. (20) into eqn. (21) and then integrating gives

$$\frac{\phi'_{11}h_1^2}{2} + \frac{\phi'_{21}h_1^2}{3} - \frac{\phi'_{1a}t^2}{2} - \frac{\phi'_{2a}t^2}{6} + f_1t - \frac{\phi'_{21}h_2^2}{2} + \frac{\phi'_{22}h_2^2}{3} = k_2 \tag{22}$$

where k_2 is a constant of integration. Using the boundary conditions at $x = \pm c$, (5)

and (11), and the fact that τ_{xya} in eqn. (14) is equal to zero at these points we find that

$$k_2 = -Q_1 = -Q_2 \tag{23}$$

This constraint imposes equilibrium in the y direction, so

$$Q_1 = Q = Q_2 \tag{24}$$

Integrating eqn. (22) gives

$$\frac{\phi_{11}h_1^2}{2} + \frac{\phi_{21}h_1^2}{3} - \frac{\phi_{1a}t^2}{2} - \frac{\phi_{2a}t^2}{6} - \phi_{12}h_2t + \frac{\phi_{22}h_2}{2} - \frac{\phi_{21}h_2^2}{2} + \frac{\phi_{12}h_2^2}{3} = -Qx + k_3 \tag{25}$$

The constant of integration, k_3, is determined by considering the boundary values of the stress functions at $x = \pm c$ in a manner similar to that employed in finding k_1 and k_2. The value k_3 is then found to be:

$$k_3 = \frac{Ph_1}{2} - M_1 - Qc$$

or

$$k_3 = \frac{-Ph_2}{2} + M_2 - Pt + Qc$$

Equating these expressions for k_3 we have the following condition which ensures moment equilibrium:

$$Q = \frac{P}{4c}(h_1 + h_2 + 2t) - \frac{1}{2c}(M_1 + M_2) \tag{26}$$

This, together with constraints (18) and (23), ensures that the joint is in a state of static equilibrium.

Eqns. (17) and (25) can be viewed as two simultaneous equations of ϕ_{1a} and ϕ_{2a} in terms of the other stress functions. Solving for ϕ_{1a} and ϕ_{2a} we get

$$\phi_{1a} = [A_1]^T\{\Phi\} \tag{27a}$$

and

$$\phi_{2a} = [A_2]^T\{\Phi\} \tag{27b}$$

where $\{\Phi\} = \{\phi_{11}, \phi_{21}, \phi_{12}, \phi_{22}, x, 1\}^T$,

$$[A_1] = \frac{1}{t^2}\begin{bmatrix} 2h_1t + 3h_1^2 \\ h_1t + 2h_1^2 \\ -4h_2t - 3h_2^2 \\ 2h_2t + 2h_2^2 \\ -6Q \\ -2Pt - 6k_3 \end{bmatrix} \qquad [A_2] = \frac{1}{t^2}\begin{bmatrix} -6h_1t - 6h_1^2 \\ -3h_1t - 4h_1^2 \\ 6h_2t + 6h_1^2 \\ -3h_2t - 4h_2^2 \\ -12Q \\ 6Pt + 12k_3 \end{bmatrix}$$

The formulation is now complete. The joint stresses have been defined in terms of four independent functions (ϕ_{11}, ϕ_{21}, ϕ_{12} and ϕ_{22}) as opposed to the two functions

used by Allman[3] and Chen and Cheng.[5] The next, and final stage, of the solution procedure is to determine these functions. This can be achieved by defining the complementary energy in terms of the stress functions. Then minimisation of the energy function will yield the stress functions. Unfortunately, a closed form solution is very difficult, if not impossible, since four, coupled fourth-order differential equations need to be solved. Therefore, a numerical solution has been sought.

3.2 Numerical Solution

As advocated by Allman,[3] the present formulation is well suited to a finite element solution. Allman has suggested a solution procedure based on an equilibrium finite element method. A similar approach has been adopted here.

For a body in plane strain,

$$\{\sigma\} = [\mathbf{D}]\{\epsilon - \epsilon_t\} \tag{28}$$

where

$$\{\sigma\} = \begin{Bmatrix} \sigma_x \\ \sigma_y \\ \tau_{xy} \end{Bmatrix} \quad \{\epsilon\} = \begin{Bmatrix} \epsilon_x \\ \epsilon_y \\ \gamma_{xy} \end{Bmatrix}$$

and $\{\epsilon_t\}$ is the thermal strain array:

$$\begin{Bmatrix} (1+\nu)\alpha\Delta T \\ (1+\nu)\alpha\Delta T \\ 0 \end{Bmatrix}$$

If the material is *linearly elastic* then [**D**] is the plane strain modulus array.

The complementary energy, U^*, may be written as

$$U^* = \frac{1}{2}\int_v \{\sigma\}^T [\mathbf{D}]^{-1}\{\sigma\}\,dv + \int_v \{\sigma\}^T\{\epsilon_t\}\,dv \tag{29}$$

Remembering that for the joint $\{\sigma\} = \{\sigma_{x1}, \sigma_{y1}, \tau_{xy1}, \sigma_{xa}, \sigma_{ya}, \tau_{xya}, \sigma_{x2}, \sigma_{y2}, \tau_{xy2}\}^T$, we can use eqns. (2), (4) and (6)–(9), (12), (14) and (19) to find arrays [**N**], {**C**(x)} and {**k**} such that

$$\{\sigma\} = [\mathbf{N}]\{\Phi\} + \{\mathbf{C}(x)\} + \{\mathbf{k}\} \tag{30}$$

where

$\{\Phi\} = \{\phi_{11}, \phi'_{11}, \phi''_{11}, \phi_{21}, \phi'_{21}, \phi''_{21}, \phi_{12}, \phi'_{12}, \phi''_{12}, \phi_{22}, \phi'_{22}, \phi''_{22}\}^T$,
{**C**(x)} is a [9 × 1] array of functions of x which are known,
{**k**} is a [9 × 1] array of constants derived from the joint geometry and loading.

Now consider the joint divided into a number of finite elements of the type shown in Figure 3. The element has a finite width, 2l, and is an adherend-adhesive-adherend "sandwich."

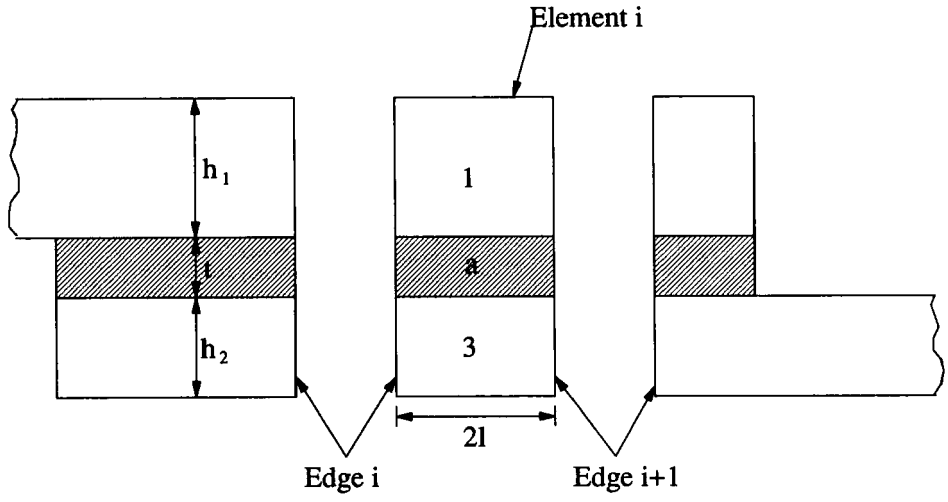

FIGURE 3 A finite element.

In this element, if edges can be viewed as "nodes" then the degrees of freedom are the stress functions and their first derivatives. Thus, each element consists of two nodes and sixteen degrees of freedom. If $\{\phi\}$ is the array of the stress functions and their first derivatives for an element with end nodes (i) and (i + 1) then:

$$\{\phi\} = \{\phi_{11}^{(i)}\ \phi'^{(i)}_{11}\ \phi_{21}^{(i)}\ \phi'^{(i)}_{21} \ldots\ldots \phi_{22}^{(i+1)}\ \phi'^{(i+1)}_{22}\}_{16\times 1}$$

We can then define an appropriate shape function array **[B]** such that

$$\{\Phi\} = [\mathbf{B}]\{\phi\} \tag{31}$$

Substitution of eqns. (30) and (31) into eqn. (29) results in the following expression for the complementary energy for an element:

$$U^{*(e)} = \frac{1}{2}\{\phi\}^T[\mathbf{F}]\{\phi\} - \{\phi\}^T[\mathbf{H}] + \text{constant}$$

If the joint is assumed to have unit width then, for each element,

$$[\mathbf{F}] = \int\int ([\mathbf{B}]^T[\mathbf{N}]^T[\mathbf{D}]^{-1}[\mathbf{N}][\mathbf{B}])\, dxdy$$

$$[\mathbf{H}] = \int\int -([\mathbf{B}]^T[\mathbf{N}]^T[\mathbf{D}]^{-1}[\{\mathbf{C}(x)\} + \{\mathbf{k}\}] + [\mathbf{B}]^T[\mathbf{N}]^T\{\epsilon_t\})\, dxdy$$

Here **[D]** is a $[9\times 9]$ matrix and is the elastic modulus array for the whole joint. The integration is taken over the whole area of the element. Explicit listings of the matrices **[B]**, **[D]**, **[F]** and **[H]** for the general case of a single lap joint with transversely isotropic adherends are given elsewhere.[8]

The total joint complementary energy is obtained by summing elemental contributions according to well-known structural analysis matrix methods. Thus, the joint complementary energy is

$$U^* = \frac{1}{2}\{\underline{\phi}\}^T[\underline{\mathbf{F}}]\{\underline{\phi}\} - \{\underline{\phi}\}^T[\underline{\mathbf{H}}] + \text{constant} \tag{32}$$

where $\{\underline{\phi}\}$, $[\underline{\mathbf{F}}]$, and $[\underline{\mathbf{H}}]$ are global matrices. The complementary energy, U^*, is minimised when

$$[\underline{\mathbf{F}}]\{\underline{\phi}\} = [\underline{\mathbf{H}}] \tag{33}$$

This is a set of linear equations which can be solved, using standard matrix methods, to give the $\{\underline{\phi}\}$ vector. For a solution to exist, $[\underline{\mathbf{F}}]$ must be a positive definite matrix. This is achieved by applying the boundary conditions (3), (5), (10) and (11) to eqn. (33). Once $\{\underline{\phi}\}$ has been obtained, the stress function at any point in the joint is determined from eqn. (31) and the stresses are calculated from eqn. (30).

3.3 The Double Lap Joint

A double lap joint (DLJ) is illustrated in Figure 4. In the present work, mid-plane symmetry will be assumed, so we need only consider one half of the joint. The DLJ differs from the SLJ in two fundamental ways. First of all, there is no *external* bending moment in the DLJ since it does not rotate like the SLJ. Secondly, due to symmetry, there is no net shear or peel force in the mid-adherend.

The formulation is similar to the SLJ case. Once again we place the x origin at the centre of the joint (Fig. 4). The coordinates y_1, y_2, y_a and stress components (σ_{x1}, σ_{y1}, τ_{xy1}), (σ_{x2}, σ_{y2}, τ_{xy2}), (σ_{xa}, σ_{ya}, τ_{xya}) refer to the upper adherend, lower adherend and adhesive respectively.

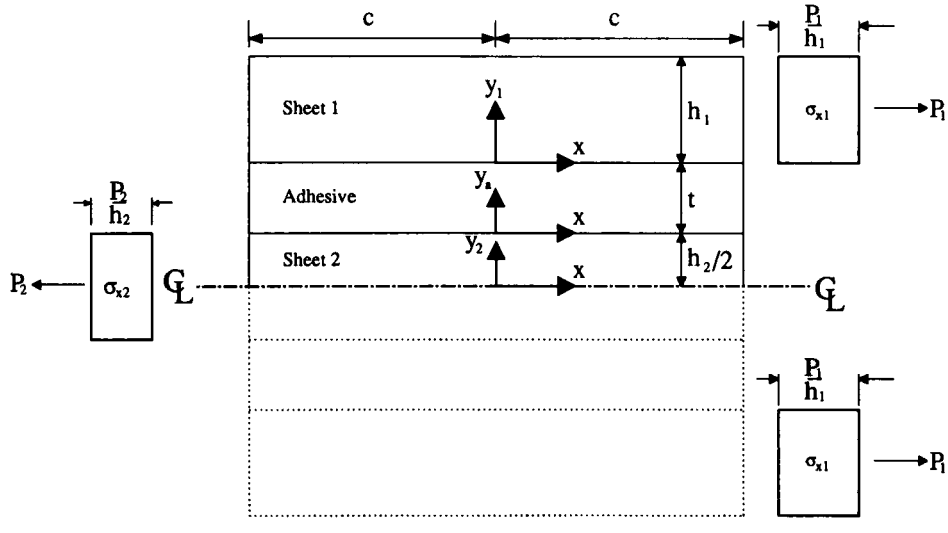

FIGURE 4 Mathematical representation of a double lap joint and its boundary conditions.

Employing the same arguments as we did for the SLJ, we find that the stress distributions in the upper adherend in the DLJ are given by

$$\sigma_{x1} = \phi_{11}(x) + \phi_{21}(x)\frac{y_1}{h_1} \tag{34}$$

$$\tau_{xy1} = \phi'_{11}(h_1 - y_1) + \phi'_{21}\left[\frac{h_1}{2} - \frac{y_1^2}{2h_1}\right] \tag{35}$$

$$\sigma_{y1} = \phi''_{11}\left[\frac{y_1^2}{2} - h_1 y_1 + \frac{h_1^2}{2}\right] + \phi''_{21}\left[\frac{y_1^3}{6h_1} - \frac{h_1 y_1}{2} + \frac{h_1^2}{3}\right] \tag{36}$$

and the edge boundary conditions are

$$\begin{bmatrix} \phi_{11} \\ \phi'_{11} \\ \phi_{21} \\ \phi'_{21} \end{bmatrix}_{x=c} = \begin{bmatrix} P_1/h_1 \\ 0 \\ 0 \\ 0 \end{bmatrix} \tag{37a}$$

$$\begin{bmatrix} \phi_{11} \\ \phi'_{11} \\ \phi_{21} \\ \phi'_{21} \end{bmatrix}_{x=-c} = \begin{bmatrix} 0 \\ 0 \\ 0 \\ 0 \end{bmatrix} \tag{37b}$$

Turning our attention to the lower adherend, let us begin with the usual assumption that the longitudinal stress is

$$\sigma_{x2} = \phi_{12} + \phi_{22}\frac{y_2}{h_2} \tag{38}$$

In this sheet there is no net applied bending moment, thus

$$\int_{-h_2/2}^{h_2/2} \sigma_{x2} y_2 dy_2 = 0$$

Substituting eqn. (38) into this condition we find that

$$\phi_{22} = 0$$

Therefore

$$\sigma_{x2} = \phi_{12} \tag{39}$$

Substituting eqn. (39) into the first equilibrium eqn. (1a) and then integrating we have

$$\tau_{xy2} = -\phi_{12}' y_2 + g_1$$

where g_1 is a function of x. However, $g_1 = 0$ if there is no net shear force in the y direction. So, we have

$$\tau_{xy2} = -\phi'_{12} y_2 \tag{40}$$

Substituting eqn. (40) into the second equilibrium eqn. (1b) gives

$$\sigma_{y2} = \phi''_{12}\frac{y_2^2}{2} + g_2 \tag{41}$$

where g_2 is a function of x. In the adhesive,

$$\sigma_{xa} = \phi_{1a} + \phi_{2a}\frac{y_a}{t} \tag{42}$$

Substituting eqn. (42) into equilibrium eqn. (1a) we get:

$$\tau_{xya} = -\phi'_{1a}y_a - \phi'_{2a}\frac{y_a^2}{2t} + g_3 \tag{43}$$

Substitution of eqn. (43) into equilibrium eqn. (1b) gives

$$\sigma_{ya} = \phi''_{1a}\frac{y_a^2}{2} + \phi''_{2a}\frac{y_a^3}{6t} - g_3'y_a + g_4 \tag{44}$$

where g_3 and g_4 are functions of x. In order to satisfy the edge conditions, the values of the stress functions at these points must be:

$$\begin{bmatrix} \phi_{12} \\ \phi'_{12} \\ \phi_{1a} \\ \phi'_{1a} \\ \phi_{2a} \\ \phi'_{2a} \end{bmatrix}_{x=c} = \begin{bmatrix} 0 \\ 0 \\ 0 \\ 0 \\ 0 \\ 0 \end{bmatrix} \tag{45a}$$

$$\begin{bmatrix} \phi_{12} \\ \phi'_{12} \\ \phi_{1a} \\ \phi'_{1a} \\ \phi_{2a} \\ \phi'_{2a} \end{bmatrix}_{x=-c} = \begin{bmatrix} P_2/h_2 \\ 0 \\ 0 \\ 0 \\ 0 \\ 0 \end{bmatrix} \tag{45b}$$

From the two shear stress interface conditions, for all x,

$$\tau_{ya}\Big|^{y_a=t} = \tau_{y1}\Big|^{y_1=0}$$

$$\tau_{ya}\Big|^{y_a=0} = \tau_{y2}\Big|^{y_2=h_2/2}$$

we have the following expressions for g_3:

$$g_3 = -\frac{\phi'_{12}h_2}{2}$$

$$g_3 = \phi''_{11}h_1 + \frac{\phi''_{21}h_1}{2} + \phi''_{1a}t + \frac{\phi''_{2a}t}{2}$$

Equating the right hand sides of these expressions and then integrating we get

$$\phi_{11}h_1 + \frac{\phi_{21}h_1}{2} + \phi_{1a}t + \frac{\phi_{2a}t}{2} + \frac{\phi_{12}h_2}{2} - k = 0 \tag{46}$$

Using the stress function boundary values (37) we get $k = P_1$ while (45) gives $k = P_2$. Therefore $P_1 = P_2$, and static equilibrium is satisfied. Applying a similar procedure as above, but using the two peel stress interface conditions, for all x,

$$\sigma_{ya}\Big|^{y_a=t} = \sigma_{y1}\Big|^{y_1=0}$$

$$\sigma_{ya}\Big|^{y_a=0} = \sigma_{y2}\Big|^{y_2=h_2/2}$$

we find that

$$g_2 = 0$$

$$g_4 = -\frac{\phi''_{2a}h_2^2}{2}$$

We can re-arrange eqn. (46) to express ϕ_{12} in terms of the other functions. This means that the entire stress condition can now be described in terms of four independent stress functions: ϕ_{11}, ϕ_{21}, ϕ_{1a}, ϕ_{2a}. These can be solved numerically employing an identical procedure to that outlined in the previous section (3.2). The **[F]** and **[H]** matrices for the double lap joint are given elsewhere.[8]

4 SOLUTION FOR AN ELASTO-PLASTIC ADHESIVE

By including initial stresses in the present formulation, an iterative scheme[9] can be used to model elasto-plasticity in the adhesive. Rewriting the stress-strain relationship (28), for the adhesive, to include initial stress $\{\sigma_i\}$, we have

$$\{\sigma\} = [\mathbf{D}]\{\epsilon - \epsilon_t\} + \{\sigma_i\} \tag{47}$$

This leads to the following definitions for the **[F]** and **[H]** matrices:

$$[\mathbf{F}] = \int\int ([\mathbf{B}]^T[\mathbf{N}]^T[\mathbf{D}]^{-1}[\mathbf{N}][\mathbf{B}])\,dxdy$$

$$[\mathbf{H}] = \int\int -([\mathbf{B}]^T[\mathbf{N}]^T[\mathbf{D}]^{-1}[\{\mathbf{C}(x)\} + \{\mathbf{k}\}] + [\mathbf{B}]^T[\mathbf{N}]^T\{\epsilon_t\} + [\mathbf{D}]^{-1}\{\sigma_i\})\,dxdy$$

where **[F]** remains unaffected but there is an extra term for initial stress in **[H]**. This extra term is easily calculated if Gaussian integration points are introduced and the initial stresses are determined at these points.

The complete process is as follows (the numbers inside the brackets refer to the load increment, outside the brackets they refer to the iteration):

(1) $[\underline{\mathbf{H}}_0]$ is assembled for the full required load level. The system $\{\underline{\phi}_0\} = [\underline{\mathbf{F}}]^{-1}[\underline{\mathbf{H}}_0]$ is solved and the $\{\underline{\sigma}_0\}$, $\{\underline{\epsilon}_0\}$ arrays are obtained. Each Gauss point is then tested for yield and the load is scaled down to a level which causes first yield.

(2) An increment of the remaining load is applied, $[\underline{\mathbf{H}}] = [\underline{\mathbf{H}}_1]_0$ is assembled and the system

$$\{\underline{\Phi}_1\}_1 = [\mathbf{F}]^{-1}[\underline{\mathbf{H}}_1]_0$$

is solved.

(3) The resulting elastic *changes* in stress $\{\delta\underline{\sigma}'_1\}_1$ and strain $\{\delta\underline{\epsilon}_1\}_1$ are determined.

(4) At each Gauss point, the actual stress increment, $\{\delta\sigma_1\}_1$, due to the strain $\{\delta\epsilon_1\}_1$ is computed in accordance with the plasticity rule

$$d\{\sigma\} = [\mathbf{D}_{ep}]d\{\epsilon\}$$

where $[\mathbf{D}_{ep}]$ is the well known elasto-plastic modulus matrix.[10] The current stress strain state is determined (and stored):

$$\{\sigma\} = \{\sigma_0\} + \{\delta\sigma_1\}_1$$

$$\{\epsilon\} = \{\epsilon_0\} + \{\delta\epsilon_1\}_1$$

(5) The difference in stress $\{\delta\sigma'_1\}_1 - \{\delta\sigma_1\}_1$ is treated as an initial stress $\{\sigma_i^{(1)}\}_1$ and used to determine a new $[\underline{\mathbf{H}}]$. $\{\sigma_i^{(1)}\}$ can be viewed as the stresses required to restore the stress to the correct plastic value (see Fig. 5).

(6) The system

$$\{\underline{\Phi}_1\}_j = [\mathbf{F}]^{-1}[\underline{\mathbf{H}}_1]_{j-1}$$

is solved and steps 3–5 repeated until the difference $\{\underline{\Phi}_1\}_{j-1} - \{\underline{\Phi}\}_j$ or the vector $\{\underline{\sigma}_i^{(1)}\}_j$ is less than a specified value.

(7) The next load increment is applied and the iterative process of steps 2–6 repeated until the full load has been applied.

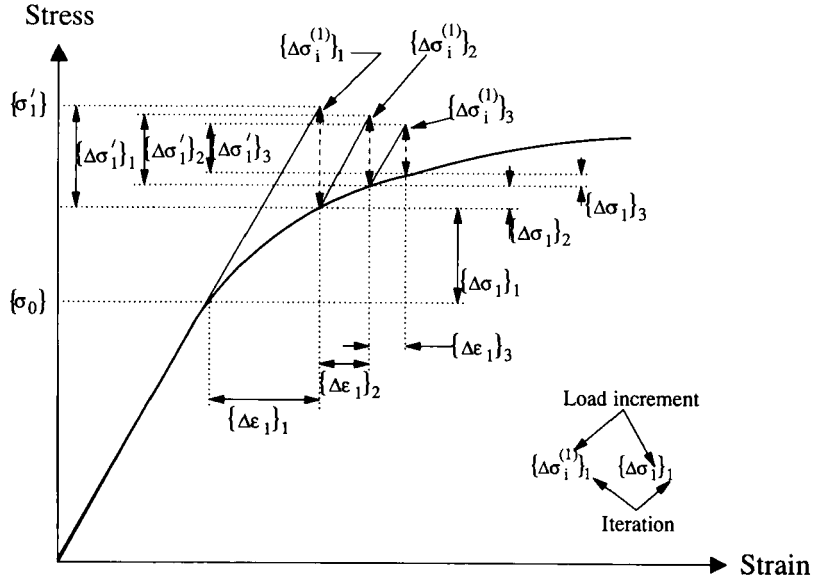

FIGURE 5 Initial stress solution procedure.

5 VALIDATION

An interactive computer program for a desktop Personal Computer, JOINT, has been developed to implement the numerical solution described above. The adhesive elastic stresses obtained for a typical Aluminium-Aluminium single lap joint are compared in Figure 6 with a Finite Element (FE) analysis, using the program FELDEP.[11] The modelled joint consisted of 1.62 mm thick and 25 mm wide adherends with an overlap of 13 mm and a glue line thickness of 0.125 mm. In the FE model, three 8-noded isoparametric elements were employed across the adhesive thickness. A load of 8.5 kN was applied to the joint. To allow comparisons between the present theory, FE and the theory by Allman,[3] the distributions have been averaged across the adhesive thickness. This has been achieved by summing all the Gauss point values across the thickness and then dividing the total by the number of Gauss points.

The present theory seems to agree well with FE except at the very ends where the FE peaks are higher and closer to the edges. Contrary to the FE predictions, the theoretical peel stresses seem to fall at the ends. However, if the peel stress at the lower adherend/adhesive interface is plotted (Fig. 7), then the theory predicts a similar trend to the FE in that the stresses fall at the unloaded end only. This example illustrates one of the dangers in plotting averaged adhesive stresses.

A far greater consequence of averaging is the loss of accuracy in joint strength prediction. This is simply because the maximum stress occurs near the adhesive/adherend corner and this value will always be higher than any average. In fact, there exists a mathematical singularity in this region[12] and even with a FE solution an accurate value of stress is difficult to obtain.

To assess the accuracy of the present theory in this critical region, principal stress vectors in the adhesive layer are compared with FE predictions in Figure 8. In this plot, vectors with bars at each end signify a compressive principal stress.

The theoretical vectors suggest a through thickness variation of stress similar to that predicted by FE. The main difference is in the magnitude and position of the peak stresses. Whereas the FE vectors peak towards the edge, the theoretical ones peak further into the overlap region, an effect which was observed earlier in Figure 6. Furthermore, the largest FE vector occurs at the adhesive/adherend corner. However, as mentioned above, there is a singularity at this point and this FE vector is far too sensitive to mesh refinement to be meaningful. Usual practise, to avoid this problem, is to allow the FE model to be plastic in this region or to introduce a spew fillet or both. Since no such singularities arise in the present solution, it is difficult to determine its accuracy from this direct comparison with FE.

It may be that, in its initial formulation, the present solution was overconstrained thus preventing a singularity and leading to lower peak stresses. Whatever the case, an alternative method of establishing the present theory's accuracy would be to compare predicted values for strength with experimental measurements.

6 CONCLUSIONS

In an attempt to provide a lap joint analysis which was as easy to use as the closed form solutions but which approached the accuracy of the finite element method

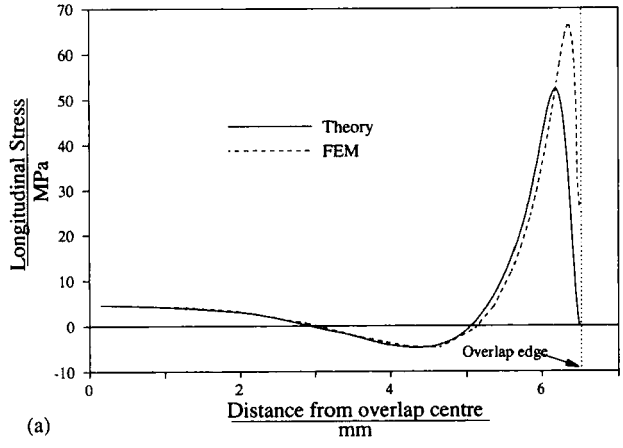

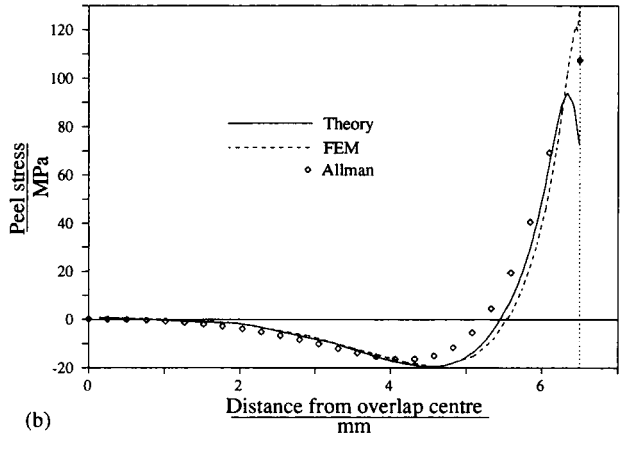

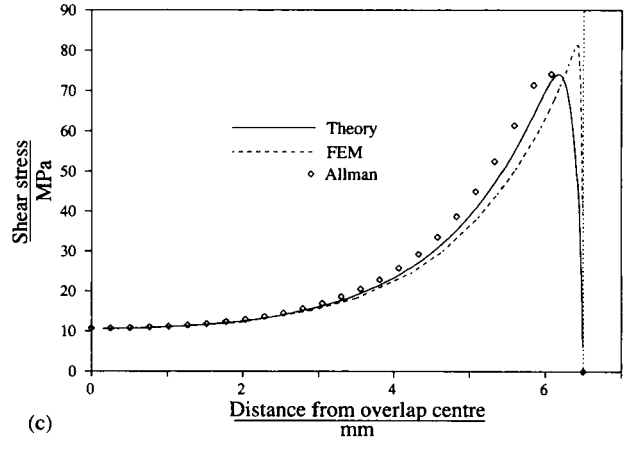

FIGURE 6 The (a) longitudinal, (b) peel and (c) shear stress distributions in an Al-Al balanced joint subjected to a load of 8.5 kN.

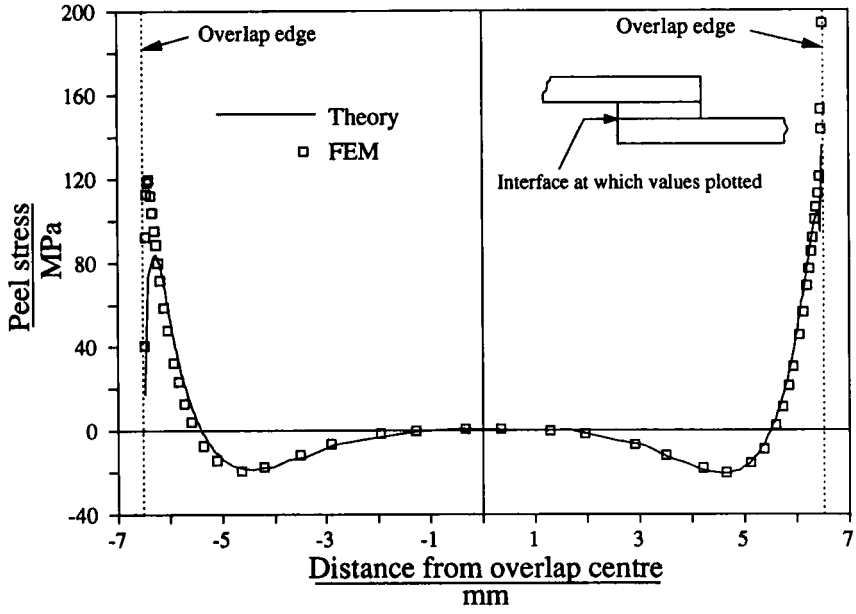

FIGURE 7 Peel stress at the adherend/adhesive interface.

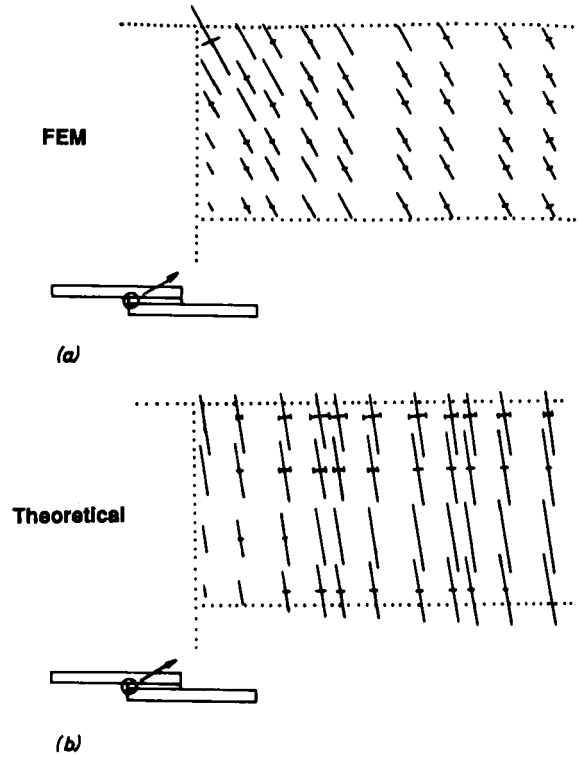

FIGURE 8 (a) FEM and (b) theoretical principal stress vectors.

(FEM), a new solution procedure has been developed. It is, in essence, an equilibrium finite element method. The finite element is an adherend-adhesive-adherend sandwich with stress as the basic variable. With the numerical nature of the method, a computer implementation of the solution is necessary. There is no disadvantage in this respect by comparison with some of the more useful closed form solutions which also require some form of computing power. The analysis improves on closed form methods by considering adhesive plasticity, in-plane (or longitudinal) stress and variation of stress through the adhesive thickness. The present method is capable of analysing a general joint consisting of dissimilar adherends of unequal thickness. In addition, thermal deformation of both adherend and adhesive is incorporated.

Comparison with FEM results showed that the present theory was in close agreement except at points close to the overlap edges. At these points, the FEM stresses are always high due to the presence of a mathematical singularity. Nevertheless, the theory agreed with the FEM regarding the nature of the stresses, if not the magnitudes, in this region.

Acknowledgements

This work was carried out with the support of the Department of Trade and Industry, and monitored by Materials and Structures Department, Defence Research Agency, (Aerospace Division).

References

1. W. J. Renton and J. R. Vinson, "Analysis of adhesively bonded joints between panels of composite materials," *J. Appl. Mech., Trans. ASME,* **44,** 101–106 (1977).
2. F. Delale, F. Erdogen and M. N. Aydinoglu, "Stresses in adhesively bonded joints—A closed form solution," *J. Composite Mat.,* **15,** 249–271 (1981).
3. D. J. Allman, "A theory for the elastic stresses in adhesive bonded lap joints," *Quart. J. of Mech. and Appl. Maths.,* **30,** (Part 4), 415–436 (1977).
4. Y. Weitsman, "Stresses in adhesive joints due to moisture and temperature," *J. Comp. Mat.,* **11,** 378–394 (1977).
5. D. Chen and S. Cheng, "An analysis of adhesive bonded single lap joints," *ASME J. Appl. Mech.,* **50,** 109–115 (1983).
6. R. D. Adams and J. A. Harris, "Strength prediction of bonded single lap joints by non-linear finite element methods," *Int. J. Adhesion and Adhesives,* **4,** (No. 2) (1984).
7. R. D. Adams, and W. C. Wake, "Structural Adhesive Joints in Engineering" (Elsevier Applied Science, London, 1984).
8. V. Mallick, "Stress analysis of metal-CFRP adhesive joints subjected to the effects of thermal stress," PhD Thesis, Dept. of Mech. Eng., University of Bristol, England (1989).
9. R. H. Gallagher and A. K. Dhall, "Direct flexibility finite element elastoplastic analysis," *Proc. Ist Int. Conf. Structural Mech.,* **Part 6,** 443–462 (1971).
10. G. C. Nayak and O. C. Zienkiewicz, "Elasto-Plastic stress analysis. A generalization for various constitutive relations including strain softening," *J. Num. Methods in Eng.,* **5,** 113–135 (1972).
11. A. D. Crocombe, "The non-linear stress and failure analysis of adhesive joints," PhD Thesis, Dept. of Mech. Eng., University of Bristol, England (1981).
12. A. D. Crocombe and R. D. Adams, "Influence of the Spew Fillet and other Parameters on the Stress Distribution in the Single Lap Joint," *J. Adhesion,* **13,** 141–155 (1981).